

X-ray spectra of two quasars at $z > 1$

K. Nandra,¹★ A. C. Fabian,¹ W. N. Brandt,¹ H. Kunieda,² M. Matsuoka,³
T. Mihara,³ Y. Ogasaka⁴ and Y. Terashima²

¹*Institute of Astronomy, Madingley Road, Cambridge CB3 0HA*

²*Department of Astrophysics, Nagoya University, Chikusa-ku, Nagoya 464-01, Japan*

³*RIKEN, Institute of Physical and Chemical Research, Hirosawa, Wako, Saitama 351-01, Japan*

⁴*Institute of Space and Astronautical Science, 3-1-1 Yoshinodai, Sagamihara, Kanagawa 229, Japan*

Accepted 1995 January 27. Received 1995 January 26; in original form 1994 September 13

ABSTRACT

We present the *ASCA* spectra of PG 1634 + 706 ($z = 1.334$) and PG 1718 + 481 ($z = 1.084$). The most striking result of our analysis is that no ‘reflection features’ – an Fe K α emission line and ‘hard tail’ – have been detected in the spectra. This contrasts markedly with the case of Seyfert galaxies, where such features are almost universal. This immediately excludes X-ray reprocessing as an origin for the (extremely luminous) blue bumps in these sources. The lack of these features is rather puzzling. In the absence of substantial X-ray beaming, we conclude that the accretion disc in these objects is either very highly ionized or optically thin. Either case might indicate that the sources are emitting close to the Eddington limit, which should cause the inner disc to expand. Furthermore, any optically thick, molecular torus, like that hypothesized in some Seyfert unification schemes, either is absent or subtends a small solid angle at the X-ray source.

Key words: accretion, accretion discs – galaxies: active – quasars: general – quasars: individual: PG 1634 + 706 – quasars: individual: PG 1718 + 481 – X-rays: galaxies.

1 INTRODUCTION

X-ray observations of Seyfert 1 galaxies have shown the signatures of reprocessing in optically thick material. The iron K α emission line and ‘hard tail’ are best explained by X-ray illumination of relatively neutral material with high column density (e.g. Guilbert & Rees 1988; Lightman & White 1988). Fluorescence in that material accounts for the emission line, and Compton scattering and absorption result in a ‘Compton reflection’ component which appears as a hard tail in the 2–30 keV spectra observed by *Ginga* (e.g. Nandra & Pounds 1994 and references therein). Several sites have been proposed for the origin of the reflection features. The most popular model is that of an accretion disc (Fabian et al. 1989; George & Fabian 1991; Matt, Perola & Piro 1991) as it fulfils the most important criteria. These are that it should remain relatively neutral, which it should if the densities are high, that it subtends a large solid angle to the source, and that it is optically thick. Other geometries, however, are not yet ruled out. For example, the features could be explained by a distribution of clouds (Guilbert & Rees 1988; Bond & Matsuoka 1993; Nandra & George 1994) or by a molecular

torus far from the nucleus, such as that postulated in Seyfert 1/2 unification schemes (Awaki et al. 1991; Ghisellini, Haardt & Matt 1994; Krolik, Madau & Życki 1994). Whatever the origin, the detection of the reflection features has considerably increased the complexity and diagnostic potential of the X-ray spectra of nearby active galactic nuclei (AGN).

In contrast, little is known about the X-ray spectra of higher-luminosity, high-redshift quasi-stellar objects (QSOs). Aside from the nearby, radio-bright quasar 3C 273 (e.g. Turner et al. 1989), the hard X-ray spectra have generally had very poor signal-to-noise ratio or spectral resolution. The IPC instrument aboard the *Einstein Observatory* provided the first large sample of QSO X-ray data (Wilkes & Elvis 1987). These results showed that the soft X-ray spectra of radio-quiet QSOs were well described by a power law without significant intrinsic absorption, and with spectral index $\Gamma \sim 2$. In some cases there was evidence for excess soft emission, identified by measurements of N_{H} lower than that expected from H I in our own Galaxy. *Ginga* provided the first reasonable hard X-ray spectra of a sample of low-redshift QSOs (Williams et al. 1992). Williams et al. found reasonable agreement with the IPC results, in that they found a correlation between radio power and X-ray spectral index, and that the radio-quiet AGN typically had slopes of $\Gamma \sim 2$. In addition they found that a few of their fits were improved

★ Present address: Laboratory for High Energy Astrophysics, Code 666, NASA/Goddard Space Flight Center, Greenbelt, MD20771, USA.

with the addition of an iron emission line or Compton reflection. In the cases where no significant features were found, the constraints were generally poor. As noted by Williams et al., however, the most significant improvements were obtained in their low-luminosity, low-redshift sources, which are really no different from the Seyferts. The exceptions to this are 3C 273 and H1821 + 643, which both showed good evidence for iron $K\alpha$ emission lines. We note, however, that the iron line in 3C 273 is very weak compared with the Seyferts, and appears to be present only in the lowest states. H1821 + 643 has a line with more typical equivalent width, but an uncertainty still remains as to whether or not the line emission arises from the surrounding cluster (Kii et al. 1991). Iwasawa & Taniguchi (1993) have presented preliminary evidence based on the *Ginga* data for an ‘X-ray Baldwin effect’, whereby the equivalent width of the iron $K\alpha$ emission line decreases with increasing luminosity. Interestingly, though, they found a significant correlation only for their ‘Seyfert’-type AGN, with the ‘quasars’ not fitting into this pattern. Most recently, Serlemitsos et al. (1994) have presented *ASCA* data for two quasars at much higher redshift ($z \sim 3$). They excluded the possibility that their X-ray spectra were reflection-dominated, as has been proposed to explain the X-ray background (Fabian et al. 1990), but no strong limits are quoted on the strength of the reflection continuum. No evidence for iron $K\alpha$ line emission were found, with upper limits to the equivalent width of 260 eV and 140 eV (assuming one interesting parameter) for their two sources. In summary, the current data regarding iron line emission and Compton reflection in QSOs are inconclusive, particularly for radio-quiet sources at high redshift.

PG 1634 + 706 ($z = 1.334$, $m_V = 14.9$) and PG 1718 + 481 ($z = 1.084$, $m_V = 15.5$) are among the most luminous QSOs in the Palomar–Green (PG) survey. As a result, they have been studied extensively at optical wavelengths. PG 1634 + 706 has also been detected in X-rays by the *Einstein Observatory* IPC (Tananbaum et al. 1986), but no reliable spectral information was obtained. Here we report on *ASCA* observations of these two PG quasars. In Section 2 we describe the data analysis method. Section 3 gives details of the X-ray spectra. Finally, in Section 4 we discuss the implications of our findings.

2 OBSERVATIONS AND DATA ANALYSIS

PG 1634 + 706 and PG 1718 + 481 were observed by *ASCA* (Tanaka, Inoue & Holt 1994) on 1994 May 1 and 1994 May 2, respectively, using both Solid-state Imaging Spectrometers (SIS0/SIS1), which are CCD detectors, and the two Gas Imaging Spectrometers (GIS) which are scintillation proportional counters (GIS2/GIS3). Special care must be taken in the analysis, particularly of the SIS data, as several factors can influence the instrumental response.

The SIS data were collected in FAINT mode with two of the four CCDs operating in each detector (see Otani et al. 1994 for further information on SIS modes and calibration issues). The data were corrected for echo – an effect whereby a small fraction of the pulse height (PH) in each event is added to the previous pixel. No correction for dark-frame error (DFE – the uncertainty in the CCD zero-level) has been applied, but these effects can be minimized by application of conservative data selection. Our selection criteria are

shown in Table 1, and were applied using the FTOOLS/XSELECT package (see Day et al. 1994 for a description of these packages and their application to *ASCA* analysis). The ELV_MIN and BR_EARTH discriminators are necessary to exclude direct contamination by the bright limb of the Earth (applicable to GIS and SIS detectors) and also to avoid increases in the DFE due to stray light in the CCDs. The DFE is also unstable for a short time after the satellite passes through the day–night terminator, becoming stable after approximately one read-out of the CCD detectors. This takes approximately 100 s in two-CCD mode. Periods when the satellite was in the South Atlantic Anomaly (SAA) and those of low GIS high voltage (HV) before and after the SAA were avoided. The discriminator on cut-off rigidity serves to reduce the background, particularly at high energies.

One further cleaning procedure is necessary for the SIS detectors. For reasons which are not currently well-understood, some of the SIS pixels show a consistently high count rate (so-called ‘hot’ pixels) and others increase in count rate from time to time (so-called ‘flickering’ pixels). These do not represent real source counts and must be removed. We applied the standard algorithm in the FTOOLS package to remove these pixels.

Proceeding to the analysis, we first extracted images for each source in each detector and chose appropriate source and background extraction cells. In all cases source counts were extracted using a circular region of varying size (typically ~ 3 arcmin) centred on the source. Background for the GIS was taken from another source-free, circular region at similar radius to the source (which is offset from the centre of the GIS field of view), and for the SIS detectors was taken from the edge of the chip. Effective areas were calculated using the current PSF and vignetting information. We used the spectral response files for the SIS released on 1994 June 20 and for the GIS on 1994 April 20. The exposure times and background-subtracted count rates following this initial analysis are shown in Table 2.

Table 1. Selection criteria.

SIS	GIS	Description
SAA = 0	SAA = 0	Outside South Atlantic Anomaly
COR_MIN > 6	COR_MIN > 7	Cut-off rigidity (GeV/c)
ELV_MIN > 7	ELV_MIN > 7	Earth elevation angle
BR_EARTH > 25	BR_EARTH > 7	Bright earth elevation
T_DY_NT > 100	–	Time between day and night terminator (s)
–	HV_RED = No	GIS HV reduced?

Table 2. Exposure times and count rates.

	SIS0	SIS1	GIS2	GIS3
PG 1634+706				
Exposure (s)	39347	39393	42668	45176
Count rate (10^{-2} ct s^{-1})	4.1 ± 0.1	2.4 ± 0.1	1.9 ± 0.1	2.5 ± 0.1
PG 1718+481				
Exposure (s)	26016	26016	30352	30350
Count rate (10^{-2} ct s^{-1})	$4. \pm 0.1$	2.4 ± 0.1	1.9 ± 0.1	2.5 ± 0.1

Source-plus-background light curves were extracted for all instruments. We found no evidence for variability of either source in any detector and thus have accumulated spectra integrated over the entire observation period. For spectral analysis, SIS PH channels 1–25 and 760–1024 were ignored, as were GIS pulse invariant (PI: gain-corrected PH) channels 1–60 and 900–1024. All remaining channels were regrouped such that there were at least 20 photons per output bin. Spectral fitting was undertaken with XSPEC 8.4.0.

3 SPECTRAL FITS

3.1 PG 1634 + 706

Spectral fitting has been initially undertaken for the four instruments separately, then, as no systematic differences in the parameters were found, the spectra were fitted together. The Galactic column density towards the direction of PG 1634 + 706 is $5.7 \times 10^{20} \text{ cm}^{-2}$, based on radio measurements (Elvis, Lockman & Wilkes 1989). Initially we have undertaken power-law fits with the line-of-sight column density, N_{H} , a free parameter, to determine whether or not the X-ray data are consistent with the value of N_{H} expected from measurements of Galactic H I. All four instruments individually (lines 1–4 of Table 3) gave a value for N_{H} compatible with that in our own Galaxy, as did the fit with all data taken together (line 5). The upper limit to the excess column density for this last fit is $4 \times 10^{20} \text{ cm}^{-2}$ if the absorber is at $z=0$, increasing to a maximum of $2 \times 10^{21} \text{ cm}^{-2}$ in the rest frame of the QSO (90 per cent limits, for two interesting parameters). This is interesting in itself, as some higher-redshift, radio-loud AGN have indicated a significant excess column (e.g. Elvis et al. 1994). It also simplifies our analysis, as henceforth we can fix the column at the Galactic value – the results of that fit are shown in Table 3. The errors quoted in this table are 68 per cent confidence for either one or two interesting parameters, depending on whether N_{H} was fixed or not ($\Delta\chi^2 = 1.0$ or 2.3). The normalization, A_{pl} , is quoted at an observed-frame energy of 1 keV. The absorption column is assumed to have zero redshift. The flux is quoted in the observed frame and is corrected for absorption. The rest-frame 2–10 keV luminosity is $8 \times 10^{45} \text{ erg s}^{-1}$, assuming $H_0 = 50 \text{ km s}^{-1} \text{ Mpc}^{-1}$ and $q_0 = 0.5$. In the full observed

band of 1–25 keV (rest frame) the luminosity is $1.7 \times 10^{46} \text{ erg s}^{-1}$.

As can be seen from line 6 of Table 3, a simple power law with Galactic absorption provides an excellent description of our data set. Fig. 1(a) shows the SIS spectra. No systematic deviations are seen in the residuals (lower panel). We note with particular interest that there is no evidence for an iron $K\alpha$ emission feature (which is expected around 2.5–3.0 keV in the observed frame), a feature which is so prevalent in Seyfert galaxies. To test this further, we have introduced a Gaussian line into the model. Henceforth we have fixed the column density at the Galactic value. We use the SIS data only, as these give far better constraints on a weak iron line. Restricting the energy to the reasonable range of 6.0–7.0 keV in the rest frame, we find that no significant improvement is obtained in the fit to either SIS spectrum separately, or when they are fitted together. The upper limit at the 90 per cent confidence level to the equivalent width of a 6.4-keV emission line with a width of $\sigma = 100 \text{ eV}$ is 120 eV (rest frame) if we use a χ^2 deviation of 2.7, appropriate for one interesting parameter (e.g. Avni 1976). Using a more conservative approach of two interesting parameters (Lampton, Margon & Bowyer 1976) we obtain an upper limit of 180 eV in the rest frame ($\Delta\chi^2 = 4.6$). The upper limits are strongly dependent on the assumed width of the line. To illustrate this, we show the confidence contours of line flux versus width in Fig. 2(a) – the confidence contours are 68 and 90 per cent for two interesting parameters. The upper limit becomes a factor of 2 worse than that given here if the width is as large as 0.5 keV.

We have also calculated an upper limit for the reflection continuum, using the model of Lightman & White (1988). We find the ratio of the reflection normalization relative to a face-on disc subtending a solid angle of 2π at the X-ray source to be $R < 0.6$, again for $\Delta\chi^2 = 2.7$, or $R < 1.0$ for $\Delta\chi^2 = 4.6$. In this fit we have used SIS and GIS detectors together. Finally, we have calculated the upper limit on R assuming the model of George & Fabian (1991), which includes the iron $K\alpha$ line assuming solar abundance and does not include Doppler or relativistic effects. From this we get the best constraints, of $R < 0.35$ or $R < 0.54$. Confidence contours for the reflection normalization $A_{\text{ref}} = RA_{\text{pl}}$ are shown in Fig. 3(a).

Finally, there is no evidence for any absorption edge in our spectra, such as might be expected from the ‘warm absorber’ (e.g. Halpern 1984), so prevalent in Seyfert galaxies (e.g. Nandra & Pounds 1994). The SIS limits are not stringent, ranging from $\tau = 0.6$ to 0.3 (90 per cent for two interesting parameters) for rest-frame edge energies between 7.1 and 9.3 keV, appropriate for the iron K absorption feature. The other strong features expected from the ionized gas are the O VII and O VIII edges (Nandra & Pounds 1992), but unfortunately these are redshifted out of the SIS energy band for our sources. Addition of a warm absorber component, which includes contributions from all elements at solar abundance (Yaqoob & Warwick 1991), provides no significant improvement in the fit.

3.2 PG 1718 + 481

Table 4 shows the spectral fits to PG 1718 + 481. A single power law is also an excellent fit to these data, whether for

Table 3. Spectral fits for PG 1634 + 706.

Inst.	A_{pl}^a	Γ^b	N_{H}	F_x (2–10 keV) ^d	χ^2_{ν}/dof
SIS0	3.18	2.00 ± 0.14	$4.4^{+3.4}_{-3.1}$	8.2 ± 1.3	1.25/83
SIS1	2.78	2.02 ± 0.21	$8.4^{+6.0}_{-5.0}$	7.2 ± 1.6	0.59/60
GIS2	2.84	2.06 ± 0.25	9^{+19}_{-9}	6.1 ± 1.0	0.70/49
GIS3	3.76	2.16 ± 0.28	23^{+21}_{-18}	7.4 ± 1.1	1.01/66
ALL	2.93	2.00 ± 0.09	$5.4^{+2.7}_{-2.3}$	7.1 ± 0.6	1.00/267
ALL	2.95	2.01 ± 0.03	5.7 (F)	7.2 ± 0.4	1.00/268

^aPower-law flux at 1 keV in the observed frame in units of 10^{-4} photon $\text{cm}^{-2} \text{ s}^{-1} \text{ keV}^{-1}$.

^bPower-law photon index.

^cEquivalent hydrogen column density (units of 10^{20} cm^{-2}).

^d2–10 keV flux in the observed frame (units of $10^{-13} \text{ erg cm}^{-2} \text{ s}^{-1}$).

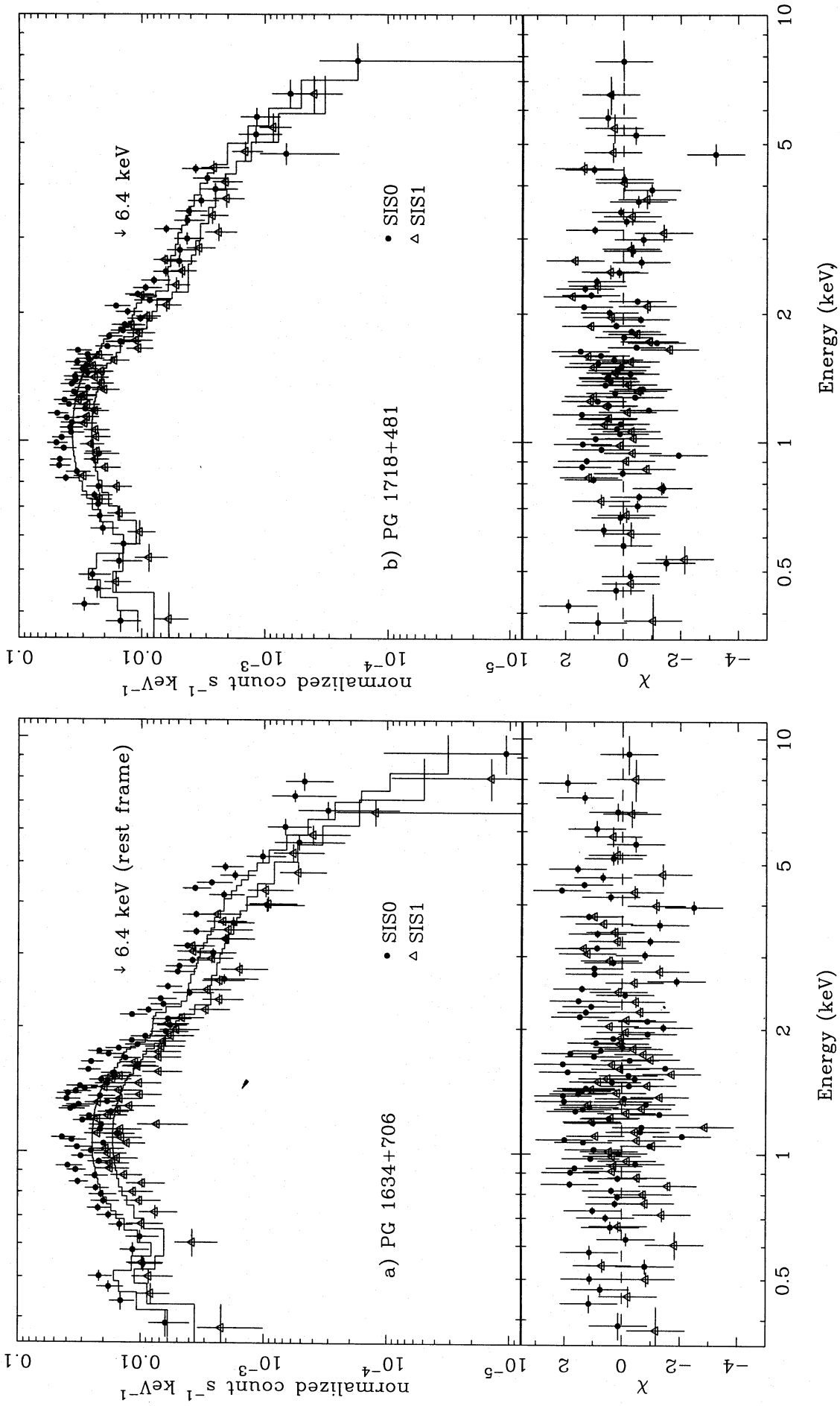


Figure 1. The ASCA SIS spectra and residuals for (a) PG 1634 + 706 and (b) PG 1718 + 481. Both sources have been fitted with a power-law model, absorbed by Galactic N_{H} . There is no evidence for further complexity. In particular, note the lack of any features around the iron K complex, at 2–3 keV (observed frame).

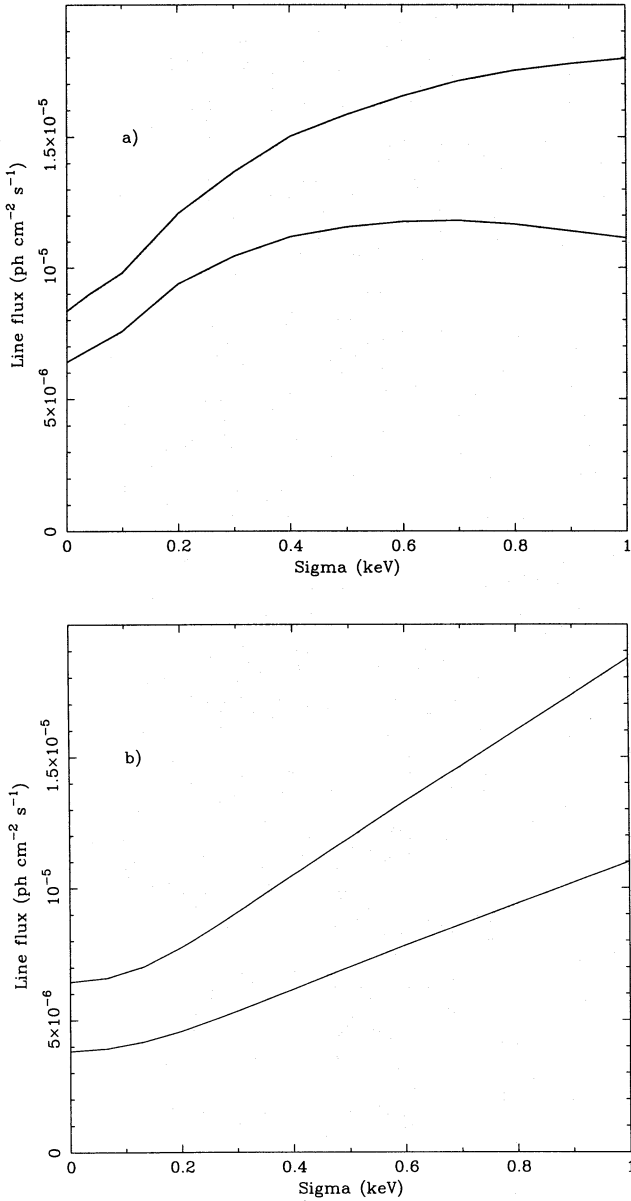


Figure 2. 68 and 90 per cent confidence contours (upper limits for two interesting parameters) for the photon flux in the line against the line width, for a Gaussian model for (a) PG 1634 + 706 and (b) PG 1718 + 481. These constraints have been obtained using only the SIS detectors, which are more sensitive to spectral features. The upper limits to the fluxes are strongly dependent on the assumed width, with higher equivalent width values being allowed if the line is broad.

the individual detectors or for all fitted together. Again, no excess absorption over the Galactic value [$N_{\text{H}}(\text{Gal}) = 2.3 \times 10^{20} \text{ cm}^{-2}$; Stark et al. 1992] is found and we have fixed the column at the H_1 value in our more complex fits. Limits on N_{H} are similar to those for PG 1634 + 706. Fig. 1(b) shows the spectrum and residuals. The luminosity is $7.6 \times 10^{45} \text{ erg s}^{-1}$ in the 2–10 keV (rest frame) band or $1.4 \times 10^{46} \text{ erg s}^{-1}$ in the full 0.8–20 keV band.

Like PG 1634 + 706, PG 1718 + 481 shows no evidence for Fe K α line emission or a spectral flattening. The limits on the equivalent width of a 6.4-keV Fe K line are even tighter,

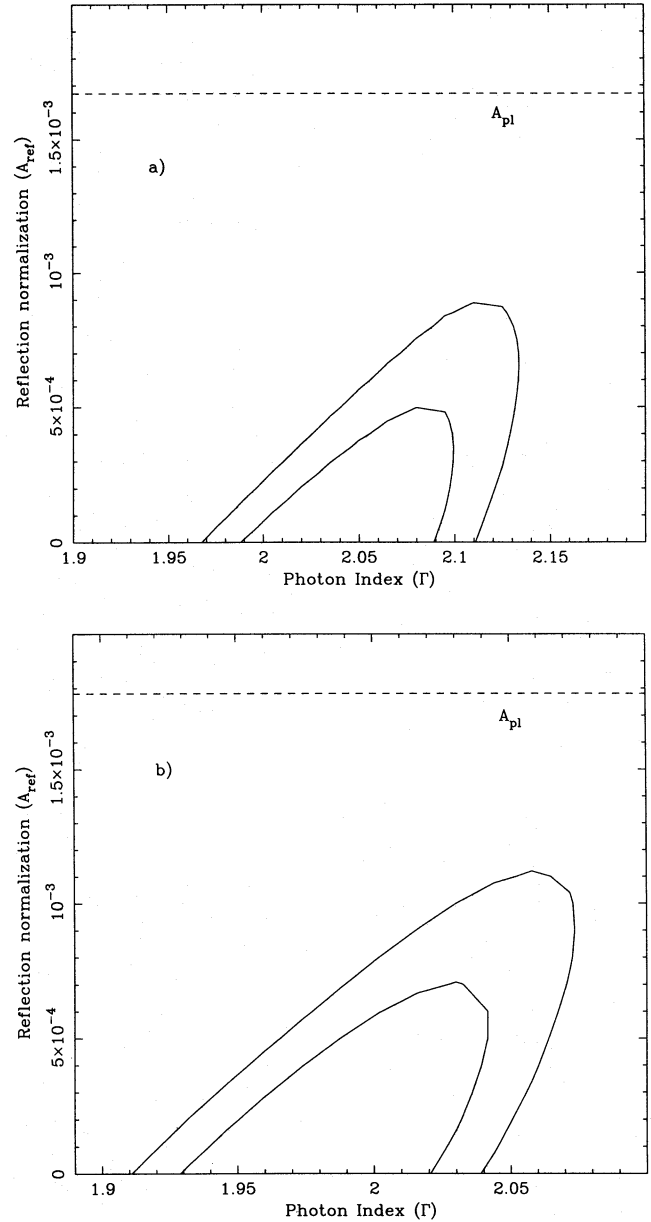


Figure 3. Upper limits to the reflection normalization A_{ref} derived from the model of George & Fabian (1991), which includes both the reflection hump and line emission from Fe K α , Fe K β and nickel K α . (a) is for PG 1634 + 706 and (b) is for PG 1718 + 481. The lines in the model are narrow compared with the resolution of the instruments (all four detectors have been employed to obtain these constraints). A_{ref} is the product of R (the ratio of the reflection component to that from a face-on accretion disc) and A_{pl} (the power-law normalization). $A_{\text{ref}} = A_{\text{pl}}$ corresponds to reflection from a face-on slab subtending solid angle 2π at the X-ray source, represented by the horizontal dashed line. This value of A_{ref} clearly excluded in both data sets.

at 85 eV or 130 eV (rest frame) for one or two interesting parameters. Again this is strongly dependent on the width, as can be seen from the confidence contours in Fig. 2(b) – in this case a σ of 600 eV is required before the upper limit doubles. The upper limits on the reflection hump are $R < 0.7$ or $R < 1.0$ for the model of Lightman & White (1988) and

Table 4. Spectral fits for PG 1718 + 481.

Inst.	A_{pl}^a	Γ^b	N_{H}^c	F_x (2–10 keV) ^d	χ^2_{ν}/dof
SIS0	4.93	2.01 ± 0.17	$3.7^{+4.3}_{-3.7}$	12.2 ± 2.2	0.75/65
SIS1	4.95	1.97 ± 0.20	$6.1^{+5.2}_{-4.3}$	13.5 ± 2.4	0.69/43
GIS2	4.12	1.94 ± 0.22	6^{+14}_{-6}	11.2 ± 2.4	0.74/66
GIS3	3.73	1.95 ± 0.21	7^{+17}_{-7}	10.2 ± 1.3	0.81/71
ALL	4.18	1.97 ± 0.08	$2.5^{+2.4}_{-2.1}$	11.0 ± 0.6	0.91/253
ALL	4.16	1.96 ± 0.03	2.3 (F)	11.2 ± 0.5	0.91/254

^aPower-law flux at 1 keV in the observed frame in units of 10^{-4} photon $\text{cm}^{-2} \text{s}^{-1} \text{keV}^{-1}$.

^bPower-law photon index.

^cEquivalent hydrogen column density (units of 10^{20}cm^{-2}).

^d2–10 keV flux in the observed frame (units of $10^{-5} \text{erg cm}^{-2} \text{s}^{-1}$).

$R < 0.45$ or $R < 0.64$ for the George & Fabian model (i.e. including constraints on both the line and continuum). Confidence contours for this last reflection fit are shown in Fig. 3(b).

Again, we find no evidence for an absorption edge from the K shell of iron, or for a warm absorber.

3.3 Multiwaveband spectra

We have constructed multiwaveband spectra of our two targets and these are shown in Fig. 4. *IRAS* fluxes are taken from Sanders et al. (1989), near-IR/optical points are from Neugebauer et al. (1987) and UV points are from Bechtold et al. (1984). The latter have been dereddened using the extinction curves of Seaton (1979) assuming the Galactic column density (see above) and the conversion to $E(B - V)$ given by Bohlin (1978). Both sources carry a large luminosity in the blue bump. From the accretion disc fits of Laor (1990), the blue bump luminosities of PG 1634 + 706 and PG 1718 + 481 are $1.4 \times 10^{48} \text{erg s}^{-1}$ and $2.4 \times 10^{47} \text{erg s}^{-1}$, respectively. The X-ray luminosities are much lower than these. Integration of the observed power-law spectra from 13.6 eV to 300 keV gives broad-band EUV/X-ray luminosities of $3 \times 10^{46} \text{erg s}^{-1}$ and $4 \times 10^{46} \text{erg s}^{-1}$ for the two sources. This fits in with the result that α_{ox} , the X-ray ‘loudness’, decreases with increasing luminosity (e.g. Worrall et al. 1987). We note that at least some Seyfert galaxies have broad-band X-ray luminosities comparable to those in the blue bump (e.g. NGC 5548: Clavel et al. 1992; Mrk 841: George et al. 1993).

4 DISCUSSION

We have observed PG 1634 + 706 and PG 1718 + 481 in approximately the same (rest) energy range as *Ginga* has observed Seyfert galaxies at $z \sim 0$ (Nandra & Pounds 1994). Those latter sources show a strong Fe K α emission line and hard tail consistent with Compton reflection from optically thick material subtending a solid angle of $\sim 2\pi$, most commonly identified with an accretion disc. In contrast, the PG quasars show no such features, indicating a clear difference between the X-ray spectra of the two QSOs and the Seyferts.

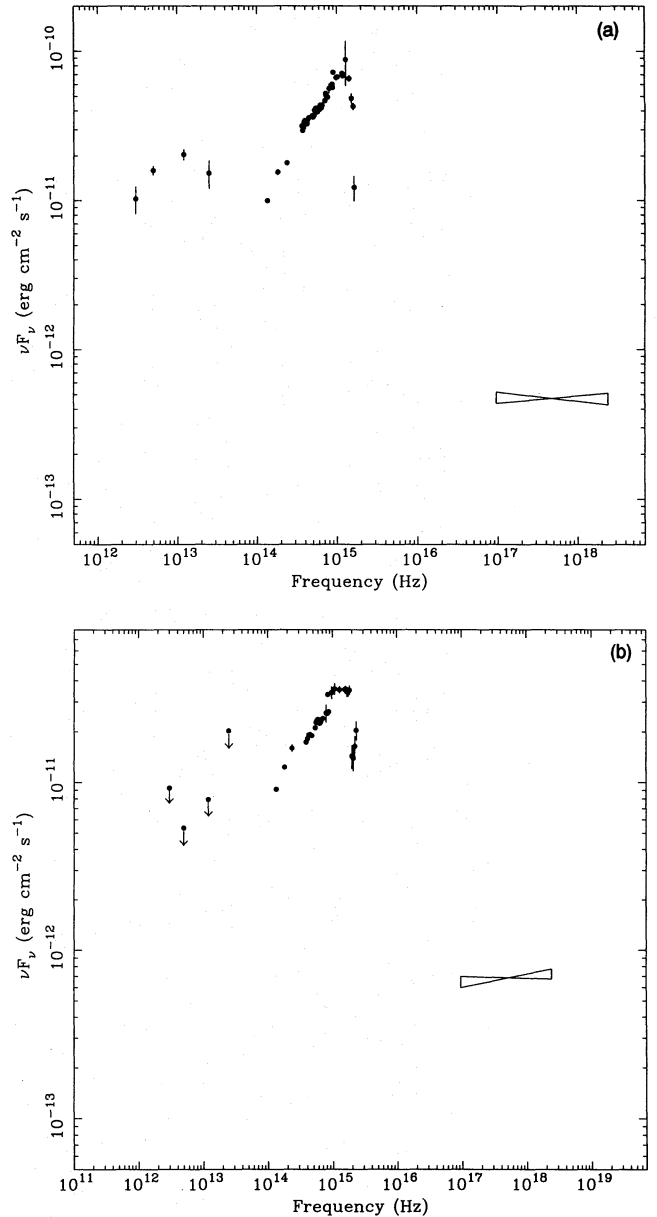


Figure 4. Multiwaveband spectra for (a) PG 1634 + 706 and (b) PG 1718 + 481, compiled from the literature but incorporating our X-ray data for the two sources (see text). The ‘bow-tie’ shows the upper and lower limits on the X-ray power law derived from spectral fitting. The excess ‘blue bump’ emission in these sources is evidently extremely strong, and the integrated luminosity in the blue bump is far greater than the observed X-ray luminosity (by a factor > 10). This and the lack of significant spectral features mean that the blue bump must be generated intrinsically, rather than arising from X-ray reprocessing.

Furthermore, the continuum spectral shapes as measured by a simple power-law fit are steeper than those for Seyferts, but very close to that inferred for the *underlying* Seyfert 1 continuum, after accounting for the reflection features, of $\Gamma = 1.95 \pm 0.05$ (Nandra & Pounds 1994). This further supports our interpretation that these sources are essentially the same as the Seyfert 1 galaxies, but without the reflection features.

One of the more important consequences of our observations is that the blue bump in these sources therefore cannot arise via reprocessing of the X-rays, a model originally suggested by Guilbert & Rees (1988). As the observed X-ray luminosity is more than a factor of 5 lower than that in the blue bump, reprocessing would only be viable either if some portion of the X-ray source were hidden from our view, e.g. by optically thick clouds, or if the X-ray emission were beamed towards the reprocessor. In either case there would be an *enhancement* of the reflection features compared with the Seyferts, which is clearly not observed.

Another conclusion of our analysis is that the parameters of any optically thick, molecular torus, such as that hypothesized in Seyfert 1/2 unification models (e.g. Antonucci & Miller 1985; Krolik & Begelman 1988), are strongly constrained. This torus has been suggested as an origin for the reflection features, as discussed by Ghisellini et al. (1994) and Krolik et al. (1994). Both sets of authors assumed an opening angle $\sim 30^\circ$ based on the observations of ionization cones in some Seyfert 2 galaxies (e.g. Pogge 1988) and estimates of the space density of Seyfert 2s compared to type 1 AGN. This implies that the torus has a large covering fraction at the X-ray source. If this were the case, the torus model would then have to be modified such that the material could be Thomson-thin, with column density $< 10^{24} \text{ cm}^{-2}$, or at least that any Thomson-thick part would subtend a small solid angle ($< \pi$) at the source. Alternatively, these QSOs may be so luminous that the torus is destroyed, as the source flux at 1 pc may be sufficient that the dust sublimation temperature of $\sim 1500 \text{ K}$ is exceeded.

The most popular model for the reflection features, that of an optically thick accretion disc, also fails for the same reason, although there is more uncertainty about the strength of the reflection features. We consider here how the accretion disc reflection model might be reconciled with the data. First, the strength of the reflection features in the disc model is a strong function of the inclination of the disc. For edge-on geometries, the reflection continuum is suppressed (George & Fabian 1991). One possibility, then, is that both these QSOs are observed edge-on (both require $i > 70^\circ$ assuming the constraints from the George & Fabian model). We consider this to be highly unlikely, recalling the fact that they are extremely luminous in the UV, and are the brightest sources above $z = 1$ in the PG sample. As these were selected based on ultraviolet excesses, the brightest objects are much more likely to be face-on. Another possibility is that the iron in these objects is at less than solar abundance. In this case the line would be reduced. We are still left with the constraints on the reflection hump, as this is largely unaffected by the iron abundance, but these are not as severe as when the two limits are combined. Although a low iron abundance remains a possibility, we note that Hamman & Ferland (1992) have suggested that the metal abundances in such QSOs may be *higher* than the solar values.

Some recent models have suggested that the disc may be ionized (Ross & Fabian 1993; Matt, Fabian & Ross 1993). In this case the line equivalent width can be either larger or smaller than in the case where the disc is neutral. Larger values are obtained because, for the most highly ionized species, the effective fluorescence yield is high. On the other hand, resonant trapping of the line in intermediate ionization states may result in a small line flux. If there is a range of ioni-

zation parameters in the disc, that might also result in the line being broader than in the case of Seyfert galaxies as, in addition to the Doppler and gravitational effects, there will be additional broadening due to line blending. As we have shown above, our limits on the line equivalent width are not as tight if the line is very broad. In addition, for a highly ionized disc the reflection component is not as prominent, as the lack of photoelectric absorption means that it has a similar shape to the illuminating continuum radiation. Ionization, however, is not necessarily an attractive interpretation for these sources, simply because the ratio of the ionizing continuum to the blue bump luminosity is a factor of ~ 10 lower than in Seyferts.

One other possibility, which is perhaps the most plausible, is that the assumption of a thin disc breaks down. As these sources are extremely luminous and have very large blue bumps, they may be accreting very close to the Eddington luminosity. Indeed, the accretion disc fit of Sun & Malkan (1989) to the IR/optical/UV spectrum of PG 1718 + 481 has a best-fitting value of \dot{M} higher than the Eddington rate. Laor (1990) found subcritical accretion rates for both objects, but still above about 25 per cent. If this is the case, we might expect the inner parts of the disc to 'puff up' due to radiation pressure. This may cause several effects which reduce the reflection component. First, the disc may become optically thin. In this case no reflection features are expected. Secondly, a thick disc would be of lower density than a standard α -disc, which would increase the ionization parameter. It is conceivable that the inner parts of such a disc (which may have a toroidal form) may form a skin of material in which even the iron is fully stripped. Furthermore, the puffed-up inner region could shield the X-ray source from the cooler, outer parts of the disc. Thus, the bulk of the reflection could come from very close to the black hole, dramatically increasing the relativistic broadening. As we have stated, we *cannot* exclude a very strong emission line if it is as broad as $\sim 1 \text{ keV}$. The corresponding Keplerian velocity is of order $100\,000 \text{ km s}^{-1}$, which is not implausible for the inner disc. The continuum would not be as strongly modified by these effects, but, if the reflecting medium is ionized, the contrast of the hump decreases substantially.

Another possibility is that the X-ray source is beamed towards us, and therefore away from the disc. This would seem reasonable in explaining the lack of any strong features in the *ASCA* spectra of PKS 0438–436 and PKS 2126–158 at $z \sim 3$ (Serlemitsos et al. 1994). Both are powerful flat-spectrum radio sources. Only a modest beaming factor of ~ 2 would be required to render the reflection features undetectable. Such a model is perhaps conceivable in the case of PG 1718 + 481, which is a moderately bright radio source ($\sim 100 \text{ mJy}$ core at 5 GHz: Kellerman et al. 1989). Both radio and X-rays might then arise in a jet. However, PG 1634 + 706 is firmly in the radio-quiet category, with a core flux of $\sim 1 \text{ mJy}$ at 5 GHz. The X-ray spectra of the two sources (and indeed the overall spectral energy distributions: Fig. 4) are extremely similar and the spectral slopes are equal to that inferred for the underlying index of Seyfert galaxies. An X-ray emission mechanism that is common to both classes and stable in spectral shape over > 4 decades in luminosity is therefore strongly indicated. Synchrotron-self-Compton jet models to explain the emission of radio-loud quasars and blazars tend to produce a

wide variety of slopes in the X-ray, as required in these objects. For radio-quiet objects, in which the X-ray spectral index lies in a narrow range around $\Gamma = 1.9$ – 2.0 , these models are much less likely.

At least two hard X-ray production mechanisms have been proposed, which *can* explain the constancy of the power-law index in radio-quiet AGN. The first invokes saturated non-thermal pair production in a plasma with high electron Lorentz factor, γ_{\max} (Zdziarski et al. 1990). A problem with this model is that recent *OSSE* observations (e.g. Johnson et al. 1994) have shown that the hard X-ray/ γ -ray fluxes of radio-quiet AGN are weak. In particular there are tight limits on the strength of any annihilation feature, which appear to rule out the high- γ_{\max} models. The *OSSE* spectra are more suggestive of a model in which electrons with a thermal distribution Compton-upscatter soft seed photons. In one such model (Haardt & Maraschi 1991, 1993), a stable photon index of $\Gamma \sim 2$ can be produced due to the balance between the energy dissipation in an accretion disc and the hot Comptonizing corona above it, as long as the optical depth is low ($\tau < 0.5$). Unfortunately, such a model explicitly predicts the reflection features from the disc, unless the optical depth in the corona is so high that they are smeared out by scattering ($\tau > 1$). Both models are based on scattering of soft seed photons. Our results clearly show that the hard X-ray photon index is largely unaffected by the energy distribution between the seed photons and the X-rays.

In summary, our results are difficult to explain in the context of accretion disc models for the source of blue bump and models of the X-ray emission in AGN. Confirmation of these results in the shape of further data on similar objects might give us cause to revise these ideas substantially.

ACKNOWLEDGMENTS

We thank the *ASCA* team for their operation of the satellite and Annalisa Celotti for useful discussions. The authors are grateful to the staff at the Laboratory for High Energy Astrophysics at NASA/Goddard Space Flight Center for providing and maintaining the *FTOOLS/XSELECT* and *XSPEC* software. KN acknowledges receipt of a SERC Research Associateship. ACF thanks the Royal Society for support. WNB thanks the United States National Science Foundation and the British Overseas Research Studentship programme.

REFERENCES

- Antonucci R. R. J., Miller J. S., 1985, *ApJ*, 197, 621
 Avni Y., 1976, *ApJ*, 210, 642
 Awaki H., Koyama K., Inoue H., Halpern J. P., 1991, *PASJ*, 43, 195
 Bechtold J. et al., 1984, *ApJ*, 281, 76
 Bohlin R. C., 1978, *ApJ*, 224, 132
 Bond I. A., Matsuoka M., 1993, *MNRAS*, 265, 619
 Clavel J., Nandra K., Makino F., Pounds K. A., Reichert G. A., Urry C. M., Wamsteker W., Peracaula-Bosch M., 1992, *ApJ*, 393, 113
 Day C. S. R., Arnaud K., Ebisawa K., Goffhelf E., Ingham J., Mukai K., White N. E., 1994, *The ABC Guide to ASCA Data Reduction*. NASA/Goddard Space Flight Center
 Elvis M., Lockman F. J., Wilkes B. J., 1989, *AJ*, 97, 3
 Elvis M., Fiore F., Wilkes B. J., McDowell J., Bechtold J., 1994, *ApJ*, 422, 60
 Fabian A. C., Rees M. J., Stella L., White N. E., 1989, *MNRAS*, 238, 729
 Fabian A. C., George I. M., Miyoshi S., Rees M. J., 1990, *MNRAS*, 242, 14P
 George I. M., Fabian A. C., 1991, *MNRAS*, 249, 352
 George I. M., Nandra K., Fabian A. C., Turner T. J., Done C., Day C. R. S., 1993, *MNRAS*, 260, 111
 Ghisellini G., Haardt F., Matt G., 1994, *MNRAS*, 267, 743
 Guilbert P. W., Rees M. J., 1988, *MNRAS*, 233, 475
 Haardt F., Maraschi L., 1991, *ApJ*, 380, L51
 Haardt F., Maraschi L., 1993, *ApJ*, 413, 507
 Halpern J. P., 1984, *ApJ*, 281, 90
 Hamman F., Ferland G. J., 1992, *ApJ*, 391, L53
 Iwasawa K., Taniguchi Y., 1993, *ApJ*, 413, L15
 Johnson W. N. et al., 1994, in Fichtel C. E., Gehrels N., Norris J. P., eds, *Proceedings of the Second Compton Symposium*. AIP, New York, p. 515
 Kellerman K. I., Sramek R., Schmidt M., Shaffer D. B., Green R., 1989, *AJ*, 98, 4
 Kii T. et al., 1991, *ApJ*, 367, 455
 Krolik J. H., Begelman M. C., 1988, *ApJ*, 329, 702
 Krolik J. H., Madau P., Życki P., 1994, *ApJ*, 420, L57
 Lampton M., Margon B., Bowyer S., 1976, *ApJ*, 208, 177
 Laor A., 1990, *MNRAS*, 246, 369
 Lightman A. P., White T. R., 1988, *ApJ*, 335, 57
 Matt G., Perola G. C., Piro L., 1991, *A&A*, 245, 75
 Matt G., Fabian A. C., Ross R. R., 1993, *MNRAS*, 262, 179
 Nandra K., George I. M., 1994, *MNRAS*, 267, 974
 Nandra K., Pounds K. A., 1992, *Nat*, 359, 215
 Nandra K., Pounds K. A., 1994, *MNRAS*, 268, 405
 Neugebauer G., Green R. F., Matthews K., Schmidt M., Soifer B. T., Bennett J., 1987, *ApJS*, 63, 615
 Otani C. et al., 1994, in *New Horizon of X-ray Astronomy*. Universal Academy Press, Tokyo, Japan, p. 655
 Pogge R. W., 1988, *ApJ*, 328, 519
 Ross R. R., Fabian A. C., 1993, *MNRAS*, 261, 74
 Sanders D. B., Phinney E. S., Neugebauer G., Soifer B. T., Matthews K., 1989, *ApJ*, 347, 29
 Seaton M. J., 1979, *MNRAS*, 187, 73P
 Serlemitsos P., Yaqoob T., Ricker G., Woo J., Kunieda H., Terashima Y., Iwasawa K., 1994, *PASJ*, 46, L43
 Stark A. A., Gammie C. F., Wilson R. W., Bally J., Linke R. A., Heiles C., Hurwitz M., 1992, *ApJS*, 78, 77
 Sun W.-H., Malkan M. A., 1989, *ApJ*, 346, 68
 Tanaka Y., Inoue H., Holt S. S., 1994, *PASJ*, 46, L37
 Tananbaum H., Avni Y., Green R. F., Schmidt M., Zamorani G., 1986, *ApJ*, 305, 57
 Turner M. J. L. et al., 1989, *PASJ*, 41, 345
 Wilkes B. J., Elvis M., 1987, *ApJ*, 323, 243
 Williams O. R. et al., 1992, *ApJ*, 389, 157
 Worrall D. M., Giommi P., Tananbaum H., Zamorani G., 1987, *ApJ*, 313, 596
 Yaqoob T., Warwick R. S., 1991, *MNRAS*, 248, 773
 Zdziarski A. A., Ghisellini G., George I. M., Svensson R., Fabian A. C., Done C., 1990, *ApJ*, 363, L1